Optical Society of America. Kent A. Murphy, Michael F. Gunther, Ashish M. Vengsarkar, and Richard O. Claus, "Fabry–Perot fiber-optic sensors in full-scale fatigue testing on an F-15 aircraft," Appl. Opt. 31, 431-433 (1992). doi: 10.1364/AO.31.000431

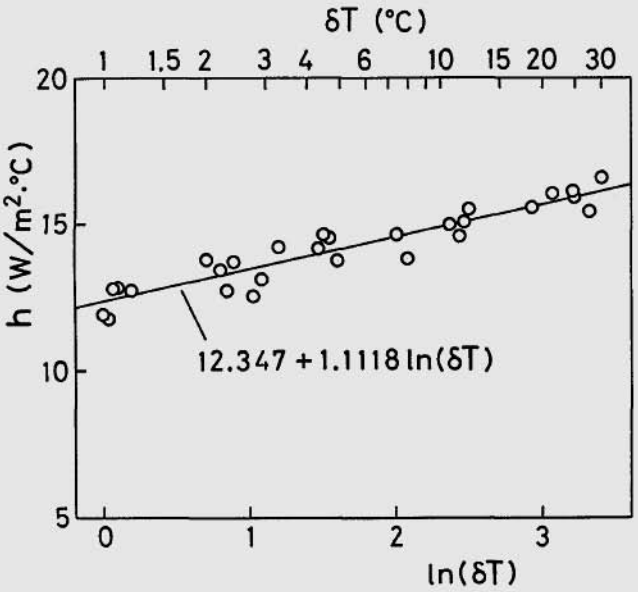

Fig. 4. Dependence of h on $\ln(\delta T)$.

The experiment was performed for $\delta T = 1 \sim 30.5$°C. Figure 3 shows the variation of $\ln|dN/dt|$ with t for $\delta T =$ 1°C and 4.5°C. The straight lines were obtained by the least-squares method. For $\delta T = 4.5$°C, we have $\mu_1 = 0.022622$ s^{-1}, and it follows that $\lambda l = l\sqrt{\mu_1/\alpha} = 0.1571$ and $h = (k/l)\lambda_i l \tan(\lambda_i l) = 14.7$ W/m$^{1/2}$ °C. Similarly, for $\delta T = 1$°C, we have $h = 12.9$ W/m^2 °C. These values fall in the range $h = 5$–30 W/m^2 °C or $h = 3$–20 W/m^2 °C for gases with free convection.[7–9] In the above calculations, we used $2l = 0.71$ mm for the effective thickness of the plate. If we simply set $2l = 2r_0 = 0.9$ mm, we have $h = 18.8$ W/m^2 °C for $\delta T =$ 4.5°C and $h = 16.4$ W/m^2 °C for $\delta T = 1$°C. Figure 4 shows the dependence of h on $\ln(\delta T)$. We see that h varies almost linearly with $\ln(\delta T)$. The results of Figs. 3 and 4 were obtained when the whole of the coil was heated uniformly. If only a portion of the coil is heated, δT for this portion is larger than that for the other, and the two portions are subjected to different cooling processes. Hence the slope of the $\ln|dN/dt|$ versus t plot will not give μ_1 of a uniformly heated coil but will give a sort of averaged value of μ_1.

We have shown that the heat-transfer coefficient of a plate can be measured by a fiber-interferometric method. A plate was modeled by a flat-coiled fiber, and the light passing the midplane of the plate detected a temperature change caused by the heat transfer between the plate and air. Since the fiber can be coiled in another shape such as a cylinder or cone, the present method may be applicable to other objects.

This work was partially supported by the Special Research Project on Energy Conversion Technology.

References

1. H. S. Carslaw and J. C. Jaeger, *Conduction of Heat in Solids* (Clarendon, Oxford, 1959), p. 120.
2. A. J. Chapman, *Heat Transfer* (Macmillan, New York, 1967), p. 131.
3. E. R. G. Eckert and R. M. Drake, Jr., *Analysis of Heat and Mass Transfer* (McGraw-Hill, New York, 1972), p. 146.
4. J. P. Holman, *Heat Transfer* (McGraw-Hill Kogakusha, Tokyo, 1976), p. 106.
5. C. J. Scott, "Transient experimental techniques for surface heat flux rates," in *Measurements in Heat Transfer*, E. R. G. Eckert and R. J. Goldstein, eds. (McGraw-Hill, New York, 1976), p. 375.
6. O. Fukumoto, ed., *Polyamide Plastics* (Nikkan Kogyo Shinbunsha, Tokyo, 1970), p. 79.
7. J. A. Adams and D. F. Rogers, *Computer-Aided Heat Transfer Analysis* (McGraw-Hill Kogakusha, Tokyo, 1973), p. 228.
8. F. M. White, *Heat Transfer* (Addison-Wesley, Reading, Mass., 1984), p. 22.
9. U. Grigull and H. Sandner, *Heat Conduction* (translated by J. Kestin, Springer-Verlag, Berlin, 1984), p. 17.

Fabry–Perot fiber-optic sensors in full-scale fatigue testing on an F-15 aircraft

Kent A. Murphy, Michael F. Gunther, Ashish M. Vengsarkar, and Richard O. Claus

The authors are with the Fiber & Electro-Optics Research Center, Bradley Department of Electrical Engineering, Virginia Polytechnic Institute and State University, Blacksburg, Virginia 24061.

Received 25 April 1991.
0003-6935/92/040431-05$05.00/0.

We report results from fiber-optic-sensor field tests on an F-15 aircraft mounted within a full-scale test frame for the purpose of fatigue testing. Strain sensitivities of the order of 0.01 μm/m have been obtained.

Fabry–Perot (FP) cavities that use Bragg gratings in or on the fiber[1] or air–glass interfaces at the fiber ends as the reflectors[2] are being used increasingly in sensing applications. A relatively new technique described by Lee and Taylor involves fabricating semireflective splices in a continuous length of fiber.[3] In a recent paper we described an optical-fiber extrinsic FP interferometer and we used it as a sensor of microdisplacements and thermally induced strain.[4]

The thrust toward fiber-optic-sensor-based smart structures and skins requires that highly stable, ruggedized sensors be available for testing in embedded or attached applications.[5] While laboratory experiments have demonstrated the applicability and potential of using stable fiber-optic sensors for in-flight monitoring systems, no results have been reported, to our knowledge, on sensors that experience gravitational forces in flight simulation studies. An important consideration in choosing a specific sensor is the format in which the final output is available. While fiber-optic sensors operated in the laboratory can be considered to be successful if output fringe patterns can be observed, practical operation can be deemed feasible only when an analog–digital output is available to the end user without having to see the fringes. Thus for this particular application, the use of fiber-based sensors and resistance-based strain gauges should be transparent to the user.

We describe results obtained from the static and dynamic loading of an F-15 mounted within a full-scale test frame for the purpose of fatigue testing at the Structures Test Facility, Wright Laboratory, Flight Dynamics Directorate, Structures Division, Wright-Patterson Air Force Base, Ohio. Extrinsic FP sensors[4] attached to the wings of the airplane

have been loaded dynamically as well as in a static fashion, and the results obtained from a software-based fringe-pattern decoding scheme are promising.

We briefly review the operation of the extrinsic FP fiber-optic sensor.[4] A single-mode fiber (λ_0 = 1300 nm), used as the input–output fiber, and a multimode fiber, used purely as a reflector, together form an air gap that acts as a low-finesse FP cavity, as shown in Fig. 1. The far end of the multimode fiber is shattered so that the reflections from the far end do not add to the detector noise. The Fresnel reflection from the glass–air interface at the front of the air gap (reference reflection) and the reflection from the air–glass interface at the far end of the air gap (sensing reflection) interfere in the input–output fiber. Although multiple reflections occur within the air gap, the effect of reflections subsequent to the ones mentioned above can be shown to be negligible. The two fibers are allowed to move in the silica tube and changes in the air-gap length cause changes in the phase difference between the reference reflection and the sensing reflection. This changes the intensity of the light monitored at the output arm of a fused biconical-tapered (FBT) coupler.

The fiber-sensor heads were attached with epoxy to the underside of the wing, ~3 ft (~1 m) from the root. Four conventional electrical strain gauges were positioned around the fiber sensors. Two fiber-sensor heads were built and assembled for use with one laser source. A single-longitudinal mode (SLM) laser diode operated at λ = 1300 nm launched light into a 2 × 2 FBT coupler. The two output arms of the coupler were concatenated to one FBT coupler each and the sensor head was attached to one of the output arms of these second-stage couplers by means of 100 m of a single-mode fiber cable. The reflections from the two sensors were detected at the photodetectors and the outputs from the detectors were connected to an oscilloscope as well as to a data acquisition system that kept track of the interference pattern. The 100-m length of fiber carried data to the simulation instrumentation room where the data acquisition system was located.

The wing was loaded from 0 to 100% in 20% increments. The 100% load is representative of an F-15 at 6,096 m (20,000 ft) with a gross weight of 17,615 kg (38,800 lb) performing a 7.0-g maneuver. A typical output plot of one of the fiber sensors for a 20–40% loading sequence is shown in Fig. 2. It was possible to deduce the strain on the wing by using a computerized data acquisition system. For this calculation, it was assumed that the attached sensor faithfully represented the strain experienced by the structure. That is, a perfect strain transfer from the wing to the fiber sensor was assumed. An elongation of 0.65 μm would then correspond to a complete fringe shift on the oscilloscope. The computerized software assumed an ideal variation in the output signal as described by the simplified equations we presented earlier.[4] We obtained a plot of the strain versus time by measuring the number of fringes as well as fractions of fringes, as shown in Fig. 3. Corresponding plots from the three electrical strain gauges matched the fiber-sensor outputs. A repetitive signal consistency was observed and data for other loading cycles was similarly obtained. The minimum detectable phase shift was 0.0996° in the linear region of the sinuosoidal transfer-function curve, which corresponds to a minimum detectable strain of 0.01 microstrains for a gauge length of 19.03 mm. In comparison, the resolution obtainable from the electrical strain gauges was ±20 microstrains at any given instant, primarily because of bridge supply noise.

Data gathered during the cyclic loading of the aircraft are instructional because the intent of the structural loading is to replicate an actual flight spectrum. A typical portion of the loading profile consists of several fluctuating load levels that represent different in-flight maneuvers and their

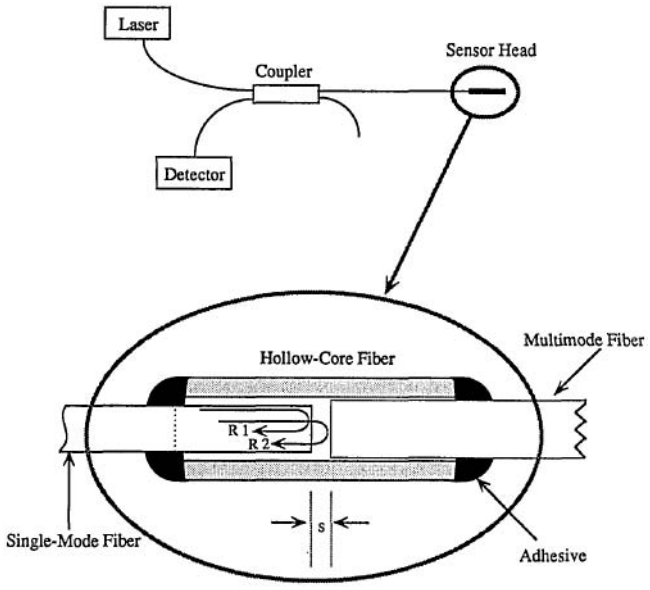

Fig. 1. Schematic of the extrinsic Fabry–Perot sensor: R1, R2, reflections from the glass–air and air–glass interfaces, respectively.

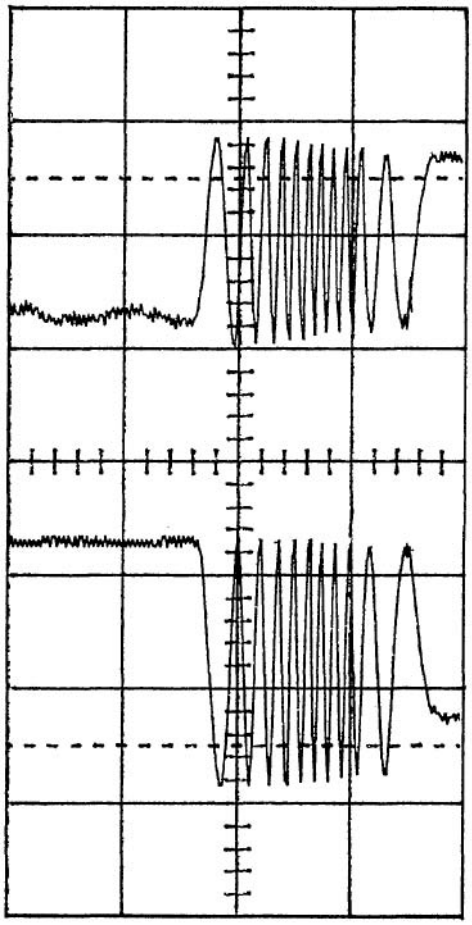

Fig. 2. Sensor output waveforms for static loading from 20 to 40% loading. Time/division; 1 s; voltage/division; 1 V.

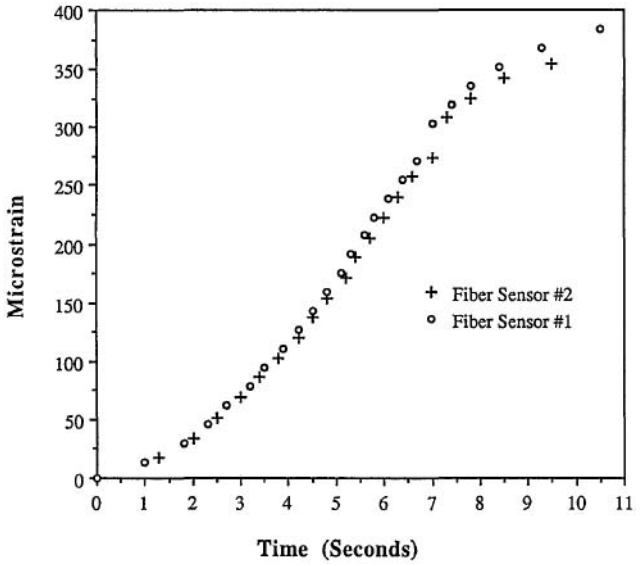

Fig. 3. Data processor output showing the variation of strain versus time. Typical output waveforms shown in Fig. 2 were fed into a software package to acquire strain information at each instant in time.

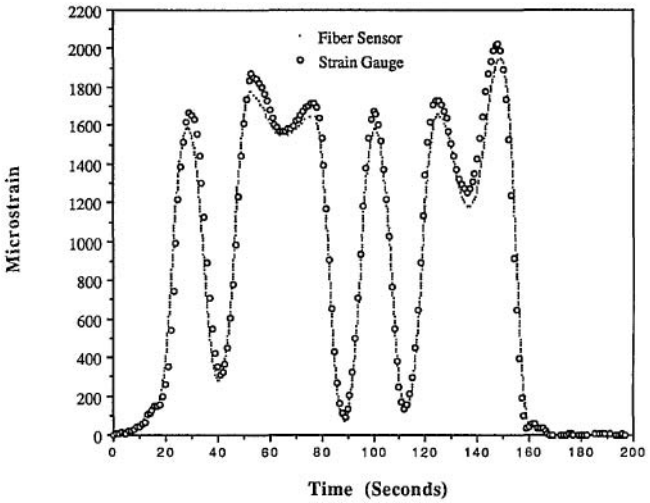

Fig. 4. Processed output showing measured strain as a function of time during the loading cycle.

associated g forces. Strain levels corresponding to the cyclic loading were obtained by using a data acquisition system. Figure 4 shows a comparison of the fiber-sensor output and the electrical strain gauge that was closest to the fiber sensor. The fiber sensor was seen to measure accurately the cyclic loading conditions with a higher resolution than the electrical strain gauges.

We have presented the first results of phase-modulated fiber-optic sensors that were externally adhered to an F-15 aircraft undergoing full-scale fatigue testing. Static and dynamic loading data obtained from the sensors show a high degree of accuracy and a strain resolution of 0.01 μm/m. The use of computerized software for decoding the output fringe pattern and the good agreement with the electrical strain gauges proves the tremendous potential of fiber sensors in practical aerospace and fiber-sensor-based smart structure applications.

We thank Clare A. Paul of the Fatigue, Fracture and Reliability Group, Structural Integrity Branch, and Ken. B. Leger of the Project Engineering Group, Structures Test Branch, for their help with the experiments at Wright Laboratory, Flight Dynamics Directorate, Structures Division, Wright-Patterson Air Force Base, Ohio. This work was supported in part by the Virginia Center for Innovative Technology.

References

1. K. L. Belsley, J. B. Carroll, L. A. Hess, D. R. Huber, and D. Schmadel, "Optically multiplexed interferometric fiber optic sensor system," in *Fiber Optic and Laser Sensors III,* E. L. Moore and O. G. Ramer, eds., Proc. Soc. Photo-Opt. Instrum. Eng. **566,** 257–265 (1985).
2. A. D. Kersey, D. A. Jackson, and M. Corke, "A simple fibre Fabry–Perot sensor," Opt. Commun. **45,** 71–73 (1983).
3. C. E. Lee and H. F. Taylor, "Interferometric optical fibre sensors using internal mirrors," Electron. Lett. **24,** 193–194 (1988).
4. K. A. Murphy, M. F. Gunther, A. M. Vengsarkar, and R. O. Claus, "Quadrature phase shifted extrinsic Fabry-Perot fiber optic sensors," Opt. Lett. **16,** 273–275 (1991).
5. A. M. Vengsarkar and K. A. Murphy, "Fiber sensors in aerospace applications: the smart structures concept," Photonics Spectra **24,** 119–124 (April 1990).

Design for an all-reflection Michelson interferometer

David D. Cleary, James W. Nichols, and D. Scott Davis

The authors are with the Department of Physics, The Naval Postgraduate School, Monterey, California 93943.
Received 1 April 1991.

We present a new design for an all-reflection Michelson interferometer that uses a concave spherical grating in an off-plane Rowland circle configuration.

Key words: *Michelson interferometer, all-reflection.*

Much of our knowledge of the Earth's upper atmosphere has been learned through observations of its ultraviolet spectrum. At low spectral resolution ($\Delta\lambda/\lambda \approx 10^{-2}$) we measure intensities of individual emissions that allow us to investigate atmospheric composition. At moderate resolution ($\Delta\lambda/\lambda \approx 10^{-4}$) we measure Doppler shifts of emission lines that allow us to analyze atmospheric dynamics. At high resolution ($\Delta\lambda/\lambda \approx 10^{-6}$) we can measure the profile of emission lines and investigate the radiation transport of optically thick lines. The latter is confined primarily to the far ultraviolet (FUV) and extreme ultraviolet (EUV) portion of the Earth's atmospheric spectrum.

For space flight observations, high-resolution measurements are made almost exclusively with interferometers rather than spectrometers. Due to the paucity of window materials in the FUV and EUV, Fabry–Perot and standard Michelson interferometers are extremely difficult, if not impossible, to build. As a result, all-reflection interferometers are sought for this portion of the spectrum. A number of designs have appeared in the literature.[1–7] These designs use plane gratings as beam splitters and, in general, require